Thermodynamic Analysis of the Interaction between a Bactericidal Antibody and a PorA Epitope of *Neisseria meningitidis*

Jean M. H. van den Elsen,[‡] Leontine M. A. van Unen,[§] Louis van Bloois,[‡] M. Antonia Busquets,[‡] Wim Jiskoot,[||] Peter Hoogerhout,[§] Jaap Wilting,[⊥] James N. Herron,[#] and Daan J. A. Crommelin*,[‡]

Departments of Pharmaceutics and Medicinal Chemistry, Faculty of Pharmacy, Utrecht Institute of Pharmaceutical Sciences, Utrecht University, Sorbonnelaan 16, 3584 CA, Utrecht, The Netherlands, Laboratories for Vaccine Research and Research on Immune Mechanisms and for Product and Process Development, National Institute of Public Health and the Environment, Anthony van Leeuwenhoeklaan 9, 3721 MA, Bilthoven, The Netherlands, and Department of Pharmaceutics and Pharmaceutical Chemistry, University of Utah, 108 Biopolymers Building, Salt Lake City, Utah 84112

Received January 8, 1997; Revised Manuscript Received April 22, 1997[⊗]

ABSTRACT: An antibody−peptide model system was used to study the binding characteristics between a bactericidal antibody (MN12H2) and the P1.16 epitope of class 1 outer membrane protein PorA of *Neisseria meningitidis* by means of a thermodynamic approach. A series of four linear peptides and three "head-to-tail" cyclic peptides (with ring sizes of 9, 15 and 17 amino acids) were synthesized and evaluated as ligands. The peptides contain a fluorescein label and the core determinant amino acid sequence TKDTNNN (residues 180−186) of the PorA P1.16 epitope of meningococcal strain H44/76. Thermodynamic data of the binding of the peptide homologs of the epitope by MN12H2 were assessed by measuring affinity constants (K_a) over a temperature range of 4−55 °C, using fluorescence spectroscopy. Curvilinear plots of ln K_a versus T (K) revealed strong temperature dependencies of enthalpy (ΔH) and entropy (ΔS). The Gibbs free energy change (ΔG) was only weakly temperature dependent. The large negative enthalpy value indicated the importance of polar interactions in the binding of both linear and cyclic peptides by MN12H2. Sturtevant's analysis of the thermodynamic parameters showed large unfavorable vibrational contributions to the binding for all linear peptides [Sturtevant, J. M. (1977) *Proc. Natl. Acad. Sci. U.S.A. 74,* 2236−2240]. The large hydrophobic contribution compensating these vibrational modes was partially attributed to aspecific interaction of the fluorescein label with the antibody. Binding of MN12H2 to conformationally restricted epitope sequences was characterized by a dramatic reduction in the size of unfavorable vibrational components of the thermodynamic parameters. Substitution of individual charged amino acids of the P1.16 epitope sequence revealed that aspartate-182 was essential for the binding. The pH profile observed for the MN12H2−peptide complexes with a midpoint pH of approximately 8.5 suggests a positively charged histidine from the antibody binding site to be involved in a charge interaction with Asp-182. These findings are consistent with the results from the crystal structure of the Fab fragment of MN12H2 in complex with a linear fluorescein-conjugated peptide homolog of the P1.16 epitope [van den Elsen et al. (1997) *Proteins* (in press)], thereby identifying the basis of an increased incidence of endemic disease in England and Wales since 1981 caused by a mutant meningococcal strain.

The Gram-negative bacterium *Neisseria meningitidis* can cause life-threatening disease in humans. Bactericidal antibodies directed against class 1 outer membrane protein PorA, such as MN12H2, have proven to play a major role in the protection against disease in an animal model (Saukkonen *et al*., 1989). All protective antibodies specific for meningococcal PorA, known so far, are directed against loop 1 or 4 of the eight cell surface exposed loops of the porin (Van der Ley *et al*., 1991). Monoclonal antibody MN12H2 is directed against epitope P1.16 situated on PorA surface loop 4 from meningococcal strain H44/76. The core determinant amino acid sequence of this epitope is TKDTNNN, residues 180−186 (McGuinness *et al*., 1990).

To investigate the interaction between bactericidal antibody MN12H2 and the P1.16 epitope, Jiskoot *et al*. (1991a) developed a method for determining the affinity constant of this antibody−antigen complex. This method is based upon the dependence of the fluorescence anisotropy of a fluorescein-labeled synthetic linear peptide, containing the core determinant of the P1.16 sequence, on the degree of binding by MN12H2. By titrating the labeled peptide with the antibody, both the affinity constant and the average number of binding sites of the complex can be determined in solution without the need of separating free and bound antigen.

Recently, the crystal structure of the Fab fragment of MN12H2 has been determined in complex with a linear fluorescein-conjugated peptide TKDTNNNL derived from P1.16 residues 180−187 (van den Elsen *et al*., 1997). The

* Address correspondence to this author at P.O. Box 80082, 3508 TB Utrecht, The Netherlands. E-mail: D.J.A.Crommelin@far.ruu.nl. Fax: +31 30 2517839.

[‡] Department of Pharmaceutics, Utrecht University.

[§] Laboratory for Vaccine Research and Research on Immune Mechanisms, National Institute of Public Health and the Environment.

[||] Laboratory for Product and Process Development, National Institute of Public Health and the Environment.

[⊥] Department of Medicinal Chemistry, Utrecht University.

[#] Department of Pharmaceutics and Pharmaceutical Chemistry, University of Utah.

[⊗] Abstract published in *Advance ACS Abstracts,* August 1, 1997.

S0006-2960(97)00043-3 CCC: $14.00

structure reveals that the peptide is bound in a type I β-turn conformation in the Fab molecule through H-bonds, van der Waals interactions, and a salt bridge.

Heretofore, much of our knowledge about antibody−antigen interactions has been provided by studies using antibodies elicited against low molecular weight haptens because it is easier to measure the antigen binding affinity for a hapten than for a protein antigen. These studies provided information not only about the driving forces behind antigen binding but also about the key contact residues that are involved in antibody−antigen complexes, using site-specific mutagenesis. Among these anti-hapten systems, the anti-fluorescein 4−4−20 system is perhaps the best characterized in solution (Herron *et al*., 1994). Only a few studies, however, describe the driving forces and the energetics of individual contact residues involved in antibody complexes with macromolecules such as peptides and proteins (Murphy *et al*., 1993, 1995; Murphy & Freire, 1995).

In this paper we describe the thermodynamic characterization of the interaction between monoclonal antibody MN12H2 and its epitope. Since the epitope sequence contains hydrophobic, polar, and charged amino acid residues, this model system offers excellent opportunities to an in-depth investigation of hydrophobic and electrostatic effects in antibody−peptide interactions.

Thermodynamic parameters of the binding of the epitope-mimicking peptides by MN12H2 were deduced from the temperature dependence of the affinity constants (K_a) of these complexes, using fluorescence spectroscopy. The relative contributions of individual amino acid residues to the overall binding could be studied by substituting single amino acids residues in the epitope. The importance of the peptide conformation was assessed by performing binding studies with "head-to-tail" cyclized peptide analogs. Our thermodynamic data are compared with the results from the crystal structure of the Fab fragment of MN12H2 in complex with the linear fluorescein-conjugated peptide.

MATERIALS AND METHODS

Mab MN12H2. Murine monoclonal antibodies were elicited against class 1 outer membrane protein epitope P1.16 of meningococcal reference strain H44/76. The antibody MN12H2 ($IgG_{2a,k}$) was purified as described by Jiskoot *et al*. (1991b). Purity of the recovered IgG fractions was assessed by SDS−PAGE, isoelectric focusing (using a Pharmacia Phast system), and gel permeation chromatography (GPC).

Peptide Synthesis. The following peptides were synthesized and derivatized with 5-(iodoacetamido)fluorescein as described by Jiskoot *et al*. (1991a): Ac-TKDTNNNLC*-NH_2, peptide 1; Ac-T**X**DTNNNLC*-NH_2, peptide 2; Ac-T**R**DTNNNLC*-NH_2, peptide 3; Ac-TK**N**TNNNLC*-NH_2, peptide 4; X = norleucyl and C* = *S*-(4-fluoresceinylcarbamoylmethyl)cysteinyl.

The synthesis and conjugation of the following cyclic peptides, cyclo[TNNNLK*TKD] (peptide C1), cyclo[AYY-TKDTNNNLTLK*P] (peptide C2), and cyclo[PAYYTKD-TNNNLTLVK*T] (peptide C3), in which K* = N^{ϵ}-[*S*-(4-fluoresceinylcarbamoylmethyl)mercaptoacetyl]lysyl, were performed as described by Brugghe *et al*. (1994) and Hoogerhout *et al*. (1995). All fluorescein-labeled peptides were purified by semipreparative HPLC, and their structural integrity was confirmed by fast bombardment mass spectrometry according to Brugghe *et al*. (1994).

Fluorescence Spectroscopy. Solutions of a fixed peptide concentration (1×10^{-7} M) were titrated with aliquots of MN12H2 in 0.01 M sodium phosphate buffer (pH 7.2) and incubated for at least 15 min, which was sufficient to reach equilibrium. Binding experiments as a function of pH were carried out in 0.01 M sodium citrate buffer (pH 8−11). Fluorescence intensity and polarization measurements of the samples were performed on an LS50 luminescence spectrometer (Perkin-Elmer Ltd., Norwalk, CT). Intensity and anisotropy were measured using an excitation wavelength of 480 nm (bandwidth 2.5 nm) and an emission wavelength of 525 nm (bandwidth 8.0 nm). Temperature measurements were carried out in a range from 4 to 55 °C using a thermostated cuvette holder. The anisotropy (A) values were computed after correction for anisotropy dependencies in the detection system (G-factor correction) as described by Herron and Voss (1981), according to the instructions of the manufacturer of the spectrometer.

The A values of bound peptide (A_{max}) were determined using a solution of 5×10^{-8} M peptide and 1.33×10^{-5} M MN12H2; higher concentrations of the antibody did not further increase the A value. In the case of peptide 4, a MN12H2 concentration up to 1×10^{-4} M was necessary to determine the A_{max} value.

Calculation of Binding Parameters. Two methods were used to determine the binding parameters of the MN12H2−peptide complexes. The first method (method 1) is based on fluorescence anisotropy measurements (Jiskoot *et al*., 1991a; Wei & Herron, 1993). This method utilizes the reduction of rotational diffusion of a small fluorescent molecule (or a nonfluorescent ligand, labeled with a fluorescent probe) upon binding to a large protein.

The fraction of fluorescence intensity (F_b) due to the bound species (peptide) is given by the equation (Bentley *et al*., 1985):

$$F_b = (A_{meas} - A_0)/(A_{max} - A_0) \quad (1)$$

where A_0 and A_{max} are the anisotropy values of the free and the bound peptide, respectively. A_{meas} is the measured anisotropy value of the MN12H2−peptide complex at a known MN12H2 concentration.

If the fluorescence intensity of the free peptide equals the intensity of the peptide in the bound state, the mole fraction of bound peptide (f_b) is the same as F_b. However, the fluorescence intensity of the fluorescein-labeled peptides was dependent of the presence of MN12H2, and hence, to calculate the bound fraction of peptide (f_b) the following equation is used (Herron, 1984; Wei & Herron, 1993):

$$f_b = F_b/[1 + Q_m(1 - F_b)] \quad (2a)$$

where Q_m is the maximum decrease in fluorescence intensity measured between the free (I_0) and the bound state (I_{max}) of the peptide resulting from eq 2b. The Q_m value is assessed similarly to the determination of the A_{max}, described above.

$$Q_m = (I_{max} - I_0)/I_0 \quad (2b)$$

Binding constants (K_a) were obtained by non-linear regression of the bound fraction (f_b) of peptide (pep) versus antibody (Ab) concentration data (saturation curve) using a two-parameter fit, as described by Wei and Herron (1993):

$$K_a = \frac{f_b}{(1 - f_b)(2[Ab] - f_b[pep])} \quad (3)$$

The second method (method 2) to determine the bound fraction of peptide is based on the decrease of fluorescence intensity (quenching) between the free and the bound state of the peptide (Wei & Herron, 1993). The fluorescence quenching (Q) is defined as

$$Q = (I_{meas} - I_0)/I_0 \quad (4)$$

where I_0 is the fluorescence intensity of free peptide and I_{meas} is the fluorescence intensity of the MN12H2−peptide complex at a known antibody concentration.

The affinity constant K_a is related to Q by the following equation as described by Wei and Herron (1993):

$$2[Ab] = \frac{K_a^{-1}Q}{Q_m - Q} + \frac{[pep]Q}{Q_m} \quad (5)$$

Calculation of Thermodynamic Parameters. Standard Gibbs free energy ($\Delta G°$) was calculated from affinity (K_a) using the equation:

$$\Delta G° = -RT \ln K_a \quad (6)$$

where R is the gas constant and T is the absolute temperature (in kelvin).

Enthalpy (ΔH^*), entropy (ΔS^*), and standard heat capacity ($\Delta C_p°$) changes were calculated by nonlinear regression analysis of affinity (K_a) versus temperature data by using a three-parameter fit based on the assumption that the $\Delta C_p°$ value is temperature independent (Gibson *et al*., 1988):

$$\ln K_a = \frac{\Delta S^* - \Delta C_p°}{R} - \frac{\Delta H^*}{RT} + \frac{\Delta C_p°}{R} \ln T \quad (7)$$

Because the values of $\Delta G°$, ΔH^*, and ΔS^* do not fully reflect the true stabilization of the antibody−antigen complex, Karush proposed the use of the concept of unitary entropy (ΔS_u) (Gurney, 1953; Pinckard, 1986). The derived equation for the determination of the unitary entropy change is

$$\Delta S_u = \Delta S° + R \ln 55.6 = \Delta S° + 33.39 \quad (8)$$

The second term (ln 55.6) is the natural logarithm of the concentration of water molecules in water ($R \ln 55.6 = 33.39$ J K^{-1} mol^{-1}) (Kauzmann, 1959). The unitary Gibbs free energy change was determined using the equation:

$$\Delta G_u = \Delta G° - 33.39T \quad (9)$$

Thermodynamic parameters were analyzed by plotting ΔG_u, ΔH^*, and $-T\Delta S_u$ versus temperature.

Calculation of Hydrophobic and Vibrational Components of Thermodynamic Parameters (Sturtevant's Analysis). Protein folding and ligand binding reduces the number of vibrational modes available to the protein, resulting in negative contributions to both entropy and heat capacity (Sturtevant, 1977). Sturtevant described an empirical method for analyzing relative contributions of both components to experimentally determined thermodynamic parameters. This analysis requires the use of unitary Gibbs free energy (ΔG_u) and entropy (ΔS_u) values instead of standard values:

$$\Delta C_p°(vib) = \frac{0.26\Delta C_p°(exp) + \Delta S_u(exp)}{1.31} \quad (10)$$

$$\Delta S_u(vib) = 1.05\Delta C_p°(vib) \quad (11)$$

$$\Delta H°(vib) = 0.53T\Delta C_p°(vib) \quad (12)$$

$$\Delta G_u(vib) = -0.52T\Delta C_p°(vib) \quad (13)$$

Hydrophobic components were determined by subtraction of vibrational components from experimental values.

Viscosity Measurements. Spherical monodisperse polystyrene "latex" particles (Dow Latex Particles, Duke Scientific, Palo Alto, CA) of different sizes (38, 198, and 624 nm) were dispersed in solutions of sucrose or (carboxymethyl)cellulose and diluted at least 10^4 times.

The diffusion coefficient (D) of these polystyrene latex spheres can be measured by dynamic light scattering as described elsewhere (Derderian, 1981; de Smidt, 1991). Dynamic light scattering experiments were performed in a Malvern PCS system (Malvern Ltd., Malvern, U.K.), equipped with a PCS4700C correlator, PCS8 photomultiplier, and a 25 mW helium/neon laser GLG5700 (NEC Corp., Tokyo, Japan). All experiments were performed at a scattering angle of 90° and at a constant temperature (4 or 25 °C). Each sample was measured six times on the basis of a 10-fold repetition measurement using the program Automeasure (version 3.2).

Viscosity Calculations. Viscosity is related to diffusion by the Stokes−Einstein equation (Hess & Klein, 1984):

$$D = kT/6\pi\eta a \quad (14)$$

where D is the diffusion coefficient, k is the Boltzman constant, T is the temperature (in kelvin), η is the viscosity, and a is the radius of the diffusing particle or molecule.

RESULTS

Linear Peptides. Linear peptide 1 was used to mimic the binding of MN12H2 to the P1.16 epitope. This peptide (Ac-TKDTNNNLC*-NH_2) contains the PorA P1.16 epitope sequence 180−187 of meningococcal strain H44/76 and an additional C-terminal cysteine residue. The latter was labeled with a thiol-reactive derivative of fluorescein [5-(iodoacetamido)fluorescein], and fluorescence polarization was used to monitor peptide binding to MN12H2 (Jiskoot *et al*., 1991a). This same approach was used to investigate the binding properties of linear peptides 2 and 3 as well. For all three linear peptides the difference between minimum and maximum limiting anisotropy (A_0 and A_{max}) was large enough to discriminate between free and bound peptide (Table 1). Neither the fluorescence intensity nor the ani-

Table 1: Binding Parameters and Affinity versus Temperature Regression Data for MN12H2 Complexed with Linear Peptides

peptide	A_0 (277 K)	A_{max} (277 K)	K_a (277 K) (M^{-1})	$\Delta G°$ (298 K) (kJ mol^{-1})	$\Delta H*$ (298 K) (kJ mol^{-1})	$\Delta S*$ (298 K) (J K^{-1} mol^{-1})	$\Delta C_p°$ (J K^{-1} mol^{-1})	bsa (Å^2)
1, TKDTNNNL	0.042 ± 0.002	0.229 ± 0.006	1.1×10^8 $\pm 0.2 \times 10^8$	−41.8	−75.0 ± 2.1	−113 ± 7	−1255 ± 295	1071
2, T**X**DTNNNL	0.038 ± 0.003	0.230 ± 0.008	4.8×10^8 $\pm 0.6 \times 10^8$	−44.4	−77.8 ± 1.1	−113 ± 4	−1238 ± 132	1057
3, T**R**DTNNNL	0.048 ± 0.002	0.248 ± 0.007	1.3×10^8 $\pm 0.2 \times 10^8$	−41.8	−84.1 ± 2.6	−144 ± 9	−1552 ± 414	1325
4, TK**N**TNNNL	0.042 ± 0.002	0.230 ± 0.01	8×10^4	(−25.9) (277 K)				

[a] The contributions of the hydrophobic effect and the change in heat capacity were calculated as described previously (Spolar et al., 1989). A conversion factor of −1.17 (±0.2) J K^{-1} mol^{-1} Å^{-2} was used to relate nonpolar buried surface area (bsa) to the heat capacity change ($\Delta C_p°$).

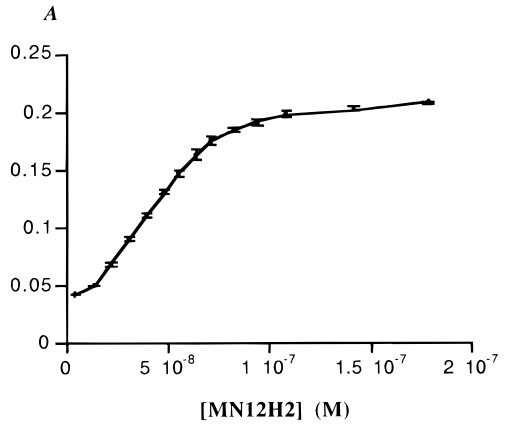

FIGURE 1: Fluorescence anisotropy (A) of peptide 1 (Ac-TKDTNNNLC*-NH_2) as a function of the MN12H2 concentration. The free peptide exhibited an anisotropy value (A_0) of 0.042(±0.002), and the anisotropy value of the bound peptide (A_{max}) was 0.229 (±0.006) (see Table 1).

sotropy value was affected by the presence of an excess of antibodies that do not bind to the P1.16 epitope. Furthermore, MN12H2 did not bind to the free fluorescent dye. However, a 28% decrease of fluorescence intensity was found between the free and the bound state of the peptide. Hence eq 2a was used to calculate the bound fraction of peptide (f_b).

Figure 1 shows a representative saturation curve for binding of MN12H2 to peptide 1 at 4 °C. The value of the affinity constant ($K_a = 1.1$ (±0.2) $\times 10^8$ M^{-1}) was derived from the saturation curve using eq 3. Subsequently, the temperature data were analyzed using a ln K_a versus temperature plot (van't Hoff analysis). The plot (Figure 2A) shows that the affinity of the complex decreases dramatically upon temperature increase. The experimental data for ln K_a were regressed against T (K) using a three-parameter model (eq 7). The regression parameters are listed in Table 1. Because 298 K is used as a reference temperature, $\Delta H*$ is equal to $\Delta H°$ and $\Delta S*$ equals $\Delta S°$. The nonlinear relationship between ln K_a and temperature indicates that the enthalpy change ($\Delta H*$) of this antibody−peptide complex is temperature dependent, which is found in most cases of protein−ligand interactions (Sturtevant, 1977). The unitary Gibbs free energy (ΔG_u), on the other hand, shows only weak temperature dependence (not shown). This is due to a compensation of the drop in $\Delta H*$ value by an increase of the $-T\Delta S_u$ value as a function of temperature. This enthalpy−entropy compensation phenomenon is known for drug−receptor interactions and for the binding of several polyclonal and monoclonal antibody with small haptens (Borea *et al.*, 1992; Gilli *et al.*, 1994; Borea *et al.*, 1995;

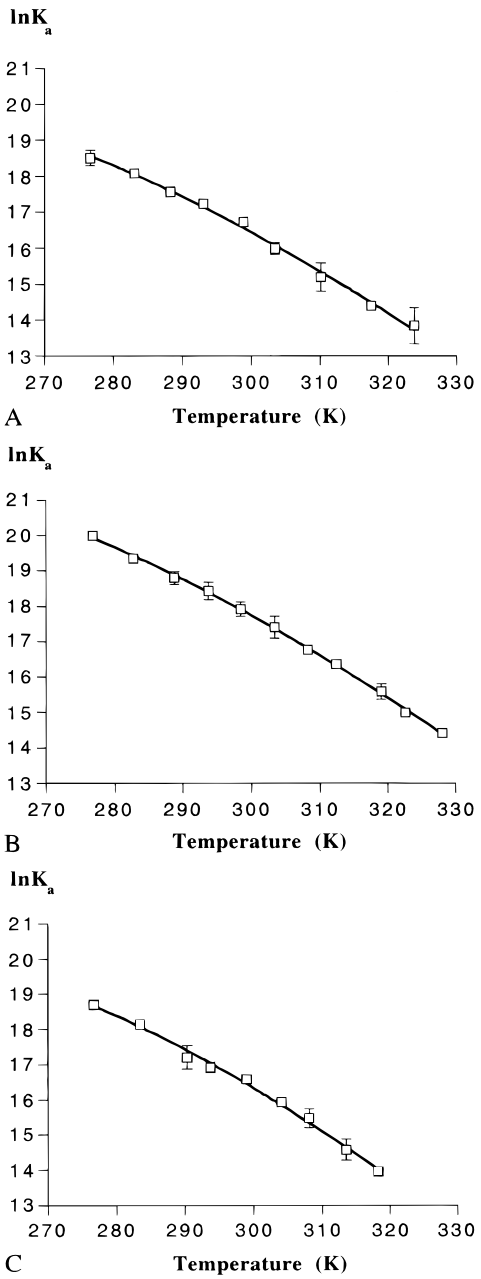

FIGURE 2: Ln K_a versus temperature plots (range: 4−55 °C) for linear peptides 1 (Ac-TKDTNNNLC*-NH_2), 2 (Ac-TXDTNNNLC*-NH_2), and 3 (Ac-TRDTNNNLC*-NH_2) (A, B, and C, respectively). Affinity constants (K_a) were calculated from fluorescence anisotropy values using eq 3. Nonlinear regression was performed using Kaleidagraph (a Macintosh program from Abelbeck Software, Inc.) according to the three-parameter fit from eq 7. Regression data are listed in Table 1. The error bars represent the standard error of at least six separate titration experiments (R-values: A, 0.998; B, 0.999; C, 0.997).

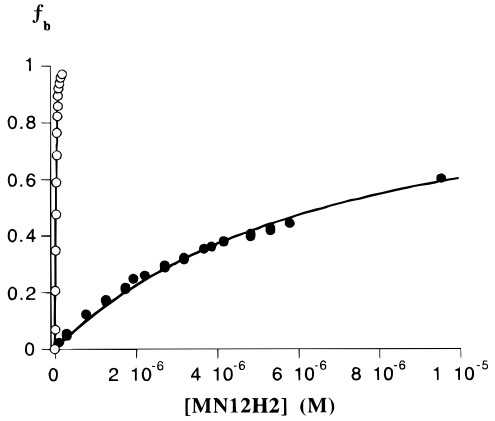

FIGURE 3: Bound fraction of peptide 1 (Ac-TKDTNNNLC*-NH_2, ○) and peptide 4 (Ac-TKNTNNNLC*-NH_2, ●) as a function of the MN12H2 concentration at 4 °C (saturation curve). Affinity constants of both complexes were calculated using eq 3: peptide 1, $K_a = 1.4\ (\pm 0.1) \times 10^8\ M^{-1}$, $R = 0.999$; peptide 4, $K_a = 8\ (\pm 1) \times 10^4$; $R = 0.995$. This plot shows the results of three separate saturation experiments for both peptides.

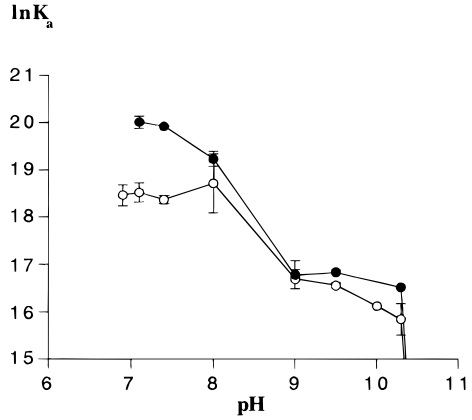

FIGURE 4: Ln K_a versus pH plot for linear peptides 1 (Ac-TKDTNNNLC*-NH_2, ○) and 2 (Ac-TXDTNNNLC*-NH_2, ●) at 4 °C. Affinity constants (K_a) were calculated from fluorescence anisotropy values using eq 3. The error bars represent the standard error of at least three separate titration experiments. Replacement of the lysine residue by an arginine (peptide 3) shows a pH dependence of ln K_a similar to that shown for peptide 1.

Mukkur, 1980; Herron *et al*., 1986), but it has not been described for antibody−peptide interactions.

Although unlikely, changes in binding affinity of the MN12H2−peptide complex with increasing temperature could possibly be due to changes in viscosity of the protein solution (which varied between 1.56 mPa·s at 4 °C and 0.81 mPa·s at 55 °C). To investigate viscosity effects on binding, the viscosity of MN12H2−peptide solutions at 4 and 25 °C was increased with sucrose or (carboxymethyl)cellulose. As expected, the affinity of the interaction did not change over the viscosity range investigated. Moreover it was found that small, temperature-related pH changes in the buffer (from 7.23 at 4 °C to 7.11 at 55 °C) did not affect the binding properties.

Amino Acid Substitutions. To investigate the role of electrostatic−polar interactions in the MN12H2−peptide complex, such as salt- or H-bridge formation, peptides were synthesized where charged amino acid residues were substituted by neutral residues. The role of the positively charged lysine-181, for instance, was studied by changing this amino acid into a hydrophobic norleucine: Ac-T**X**DTNNNL-C-NH_2 (peptide 2, X = norleucine). Binding studies (shown in Figure 2B and Table 1) indicated that this replacement resulted in a 4-fold increase in affinity at 4 °C [$K_a = 4.8\ (\pm 0.6) \times 10^8\ M^{-1}$] compared to the native epitope peptide. The temperature plot (Figure 2B) and thermodynamic parameters ($\Delta G° = -44.4$ kJ mol^{-1}, $\Delta H^* = -77.8$ kJ mol^{-1}; Table 1) obtained for peptide 2 were similar to those obtained for peptide 1, a trend which was also observed when arginine was substituted for lysine in peptide 3 (Ac-TRDTNNNL-C-NH_2) as is shown in Figure 2C.

The second charged residue of the MN12H2 epitope, aspartate-182, was changed to asparagine in peptide 4: Ac-TK**N**TNNNL-C-NH_2. Binding studies at 4 °C show very weak binding (Figure 3). The affinity constant for this complex [$K_a = 8\ (\pm 1) \times 10^4\ M^{-1}$] is 3−4 orders of magnitude lower than that for the MN12H2 complex with peptide 1 (Table 1). Subsequently, the possible role of the charged amino acid residues Lys-181 and Asp-182 in an electrostatic interaction with MN12H2 was studied by measuring the affinity constant of MN12H2 for peptides 1, 2, and 3 as a function of pH. The complex of MN12H2 with peptide 1 showed no significant change in affinity when the pH was increased from pH 6.8 to pH 7.9 (Figure 4). Between pH 8 and pH 10 the affinity of the complex decreased dramatically. At pH values higher than 10 a total collapse of the affinity constant occurred. Titration studies with peptides 2 (Figure 4) and 3 showed similar pH profiles.

Sturtevant's Analysis. To analyze the relative contribution of the hydrophobic and vibrational components of separate thermodynamic parameters, these components were computed using eqs 10−13 according to the method described by Sturtevant (1977). Sturtevant reported that the entropy changes in protein−ligand interactions were much smaller than expected on the basis of the hydrophobic effect. He ascribed the discrepancy to the loss of vibrational entropy of the protein due to the binding of the ligand. For all the complexes with linear peptides the compensation of the hydrophobic effect by intramolecular vibrational modes (at 25 °C) is listed in Table 2.

The data shown in Table 2 demonstrate large negative vibrational contributions to both the entropy value and the heat capacity of all MN12H2−linear peptide complexes. These unfavorable vibrational modes are compensated in all cases by favorable hydrophobic contributions to the binding. The MN12H2−peptide 2 complex shows a slight increase in the hydrophobic component of $\Delta G°$ and ΔH^* compared to the MN12H2−peptide 1 complex. Substitution of the lysine by a bulkier arginine residue resulted in a significant increase of the compensational effect.

Cyclic Peptides. Recently, methods were developed for synthesis and selective conjugation of "head-to-tail" cyclic peptides of 7−17 residues (Brugghe *et al*., 1994; Hoogerhout *et al*., 1995). This offered the opportunity of investigating conformational aspects of the binding of MN12H2 to the P1.16 epitope. Cyclic peptides of 9, 15, and 17 amino acid residues were used in this study. The peptides contain an N^{ϵ}-(*S*-acetylmercaptoacetyl)lysyl residue, lysine(SAMA), which enabled a selective conjugation with 5-(iodoacetamido)fluorescein. Fluorescein is attached to monitor peptide binding through changes in fluorescence polarization and/or intensity and is positioned opposite to the sequence corresponding to the epitope.

Table 2: Sturtevant's Analysis of Vibrational and Hydrophobic Contributions to the Binding of MN12H2 with Linear Peptides

peptide	$\Delta C_p°$ (298 K) (J K^{-1} mol^{-1})	ΔS_u (298 K) (J K^{-1} mol^{-1})	$\Delta H°$ (298 K) (kJ mol^{-1})	ΔG_u (298 K) (kJ mol^{-1})
		Vibrational Components		
1, TKDTNNNL	−310	−326	−48.9	48.1
2, T**X**DTNNNL	−305	−322	−48.5	47.3
3, T**R**DTNNNL	−389	−413	−61.9	61.1
		Hydrophobic Components		
1, TKDTNNNL	−946	246	−26.4	−100.0
2, T**X**DTNNNL	−933	243	−29.3	−101.7
3, T**R**DTNNNL	−1159	302	−22.2	−113.0

Table 3: Sturtevant's Analysis of Vibrational and Hydrophobic Contributions to the Binding of MN12H2 with Cyclic Peptides

peptide	$\Delta C_p°$ (298 K) (J K^{-1} mol^{-1})	ΔS_u (298 K) (J K^{-1} mol^{-1})	$\Delta H°$ (298 K) (kJ mol^{-1})	ΔG_u (298 K) (kJ mol^{-1})
		Vibrational Components		
C2, c[AYYTKDTNNNLTLKP]	−129	−136	−2.0	2.0
		Hydrophobic Components		
C2, c[AYYTKDTNNNLTLKP]	−482	125	−50.3	−51.3

Prior to the binding experiments the difference between the A_0 and A_{max} of the peptides was established, as described in the Materials and Methods section, to determine whether these values were large enough to obtain a measurable discrimination between free and bound peptides. "Head-to-tail" cyclization of the slightly extended core determinant P1.16 sequence (peptide C1) revealed no detectable change in anisotropy value upon addition of antibody MN12H2. The 15 amino acid cyclic peptide (peptide C2) showed a large enough difference between minimum ($A_0 = 0.080$ at 4 °C) and maximum anisotropy value ($A_{max} = 0.190$ at 4 °C) to perform further polarization measurements. The difference between minimum and maximum limiting anisotropy of the largest peptide (peptide C3) ($A_0 = 0.056$; $A_{max} = 0.070$ at 4 °C) was insufficient for calculation of binding parameters using method 1. Affinity constants of this peptide could be obtained by exploiting its Q_m value of −0.28, using method 2.

Both peptides C2 and C3 show an affinity constant of 3.5 (±0.6) × 10^7 M^{-1} (at 4 °C) in complex with MN12H2. Analysis of ln K_a data versus temperature data of peptide C2 (not shown) demonstrates a comparable temperature dependence as was found for linear peptides, revealing only a small decrease of Gibbs free energy ($\Delta G° = -39.3$ kJ mol^{-1}). In contrast with the linear peptides a significant decrease of the enthalpy value [$\Delta H* = -52.3$ (±1.0) kJ mol^{-1}, at 25 °C] is observed for peptide C2. The entropy value [$\Delta S* = -44$ (±3) J K^{-1} mol^{-1}, at 25 °C] as well as the results from Sturtevant's analysis of the MN12H2−peptide C2 complex (Table 3) reveals significantly less dampening of unfavorable intramolecular vibrational and rotational motions due to binding of the peptide compared to linear peptides.

Since the enthalpy values of the linear peptides and peptide C2 were so different, the cyclic peptides were not pursued further.

DISCUSSION

In this paper we describe a monoclonal antibody−peptide model system for determining the driving forces behind the binding of the P1.16 epitope of meningococcal PorA by MN12H2. By substituting selected epitope amino acid residues the relative contribution of these individual amino acid residues to the overall binding is determined.

Thermodynamic analysis of the antibody−peptide interactions reveals a large negative enthalpy change (ΔH), a negative entropy change (ΔS), and a significant negative value of heat capacity change (ΔC_p). These observations agree partly with results from calorimetric titration studies with another antibody−peptide system involving the peptide−hormone angiotensin II (Murphy & Freire, 1995), where a modest positive entropy value was observed. The negative sign of the entropy value as well as the heat capacity ($\Delta S* = -113$ J K^{-1} mol^{-1}, $\Delta C_p° = -1255$ J K^{-1} mol^{-1}, at 25° C) of the MN12H2−peptide 1 complex indicates dampening of intramolecular vibrational and rotational motions due to binding of the peptide, accompanied by a reduced solvent exposure of nonpolar groups of both the peptide and the antigen binding site.

Processes that involve phase transfer, including protein folding, protein aggregation/association, and protein−ligand binding, are characterized by large negative standard heat capacity changes ($\Delta C_p° << 0$) (Sturtevant, 1977). The large negative heat capacity values furthermore suggest a "cavity"-type binding site. The value of the buried surface area (bsa), involving nonpolar constituents, is correlated to the hydrophobic effect and therefore to the heat capacity (Chotia, 1974; Eisenberg *et al*., 1984; Rose *et al*., 1985; Spolar *et al*., 1989; Makhatadze & Privalov, 1990; Privalov & Makhatadze, 1990; Sharp *et al*., 1991; Herron *et al*., 1994). Spolar and co-workers (1989) obtained a conversion factor that correlates the change in water-accessible, nonpolar surface area to the heat capacity change [$\Delta C_p° = -1.2$ (±0.2) J K^{-1} mol^{-1} Å^{-2}]. The deeper the pocket, the more water is excluded from the binding site upon binding, resulting in a greater loss of heat storage. The nonpolar bsa of the MN12H2−peptide 1 complex (1071 Å^2) is in agreement with reported total bsa values (polar and nonpolar) ranging from 300 to 1700 Å^2 determined from a series of X-ray structures of antibody−antigen complexes (Davies *et al*., 1991). However, for Fab−peptide complexes average total bsa values of about 1000 Å^2 are reported (Davies *et al*., 1991; Wilson & Stanfield, 1993). This could imply that, apart from the binding of peptide 1 by MN12H2, the fluorescein label is involved in

a hydrophobic interaction with the antibody molecule, thereby increasing the nonpolar bsa of the complex. These findings are consistent with recent X-ray analysis of the complex between the MN12H2 Fab fragment and peptide 1 (van den Elsen *et al*., 1997). Supportive experimental evidence was obtained through a competitive binding experiment with labeled peptide 1 and unlabeled peptide 1 (missing the fluorescein label). Binding affinity of the unlabeled peptide 1 by MN12H2 was 4-fold reduced compared to the fluorescein-labeled peptide [$K_a = 2.5\ (\pm 0.1) \times 10^7\ M^{-1}$ vs $1.1\ (\pm 0.2) \times 10^8\ M^{-1}$ (at 4 °C), respectively].

The large negative enthalpy value ($\Delta H^* = -75.3$ kJ mol^{-1} at 25 °C; see Table 1) revealed by the MN12H2−peptide 1 complex indicates that polar interactions play a major role. An important source of negative contribution to $\Delta H°$ (and $\Delta S°$) will arise if a hydrogen bond is formed in an environment of low dielectric constant like an antibody combining site (Pimentel & McClellan, 1971; Omelyanenko *et al*., 1993; Herron *et al*., 1994). However, it is generally accepted that there is only marginal net free energy difference when existing H-bonds between amino acids and solvent molecules in an aqueous environment are exchanged by hydrogen bonds upon complex formation (Ross & Subramanian, 1981). Hence, hydrogen bonds formed in a low dielectric environment such as the water-inaccessible interior of the antigen binding site of MN12H2 can make substantial negative contributions to both enthalpy and entropy. Considering the peptide sequence, there are a number of possibilities for these H-bond interactions. The Gibbs free energy value ($\Delta G° = -41.8$ kJ mol^{-1}, at 25 °C) could account not only for the formation of four new H-bonds but also for the formation of two salt links.

Substitution of the charged residues of the epitope, based on the assumption that polar interactions are the major driving force governing the interaction between MN12H2 and peptide 1 (as indicated above), demonstrates that the ϵ-amino group of the Lys-181 residue of the peptide is not essential for the formation of the complex. The 5-fold increase of affinity due to the introduction of the hydrophobic side chain in the peptide (Nle instead of Lys) might be a result of the reduced size of unfavorable vibrational contribution and the increased hydrophobic effect due to the absence of a charge on the Nle residue. The exchange of Lys-181 by an arginine reveals some striking differences in the limiting anisotropy values compared to peptides 1 and 2 (Table 1). According to these values the positively charged arginine seems to be able to polarize the fluorescein molecule in the free as well as in the bound state of the peptide. The increased polarization of the label by the arginine residue might be induced by an electrostatic interaction between the positively charged guanido group of arginine and fluorescein's negatively charged benzoyl or xanthenone ring. Another possible explanation is hydrophobic stacking of this guanido group with the xanthenyl moiety of the label. Nonpolar bsa values of this complex show that the introduction of the bulky arginine group induces an increase in the nonpolar antibody−peptide contact surface (bsa: 1325 Å^2). Together with the observation of increased polarization of the label in the MN12H2−peptide 3 complex, the increased nonpolar bsa value suggests an even larger contribution of the fluorescein molecule to the contact surface than in the complexes with peptides 1 and 2.

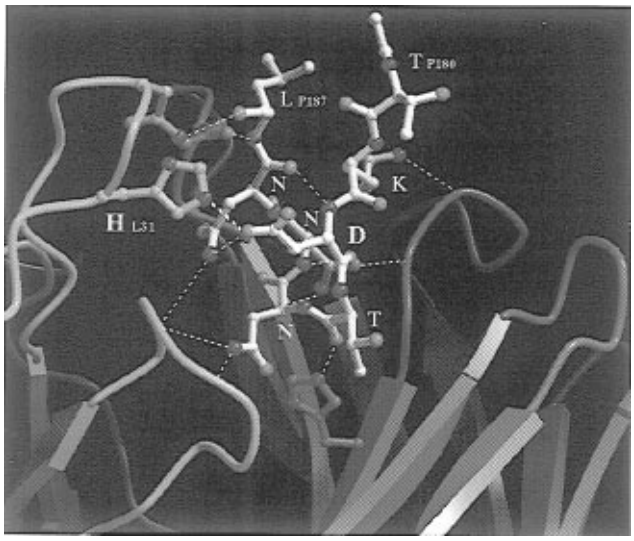

FIGURE 5: Ribbon representation of the MN12H2 antigen binding site as seen in the crystal structure of the Fab fragment of the antibody in complex with fluorescein-conjugated peptide Ac-TKDTNNNLC*-NH_2 (van den Elsen *et al*., 1997). The antigen binding site is formed by residues from hypervariable loops L1 and L3 from the MN12H2 light chain (shown in green) and hypervariable loops H1, H2, and H3 from the heavy chain (shown in purple). The peptide (shown in yellow) is folded deeply into the cavity of the binding site in a type I β-turn. Polar interactions between the Fab molecule and the peptide, including the salt bridge between peptide residue Asp-P182 (shown in white) and MN12H2 residue His-L31, are indicated by dotted lines. The figure was prepared using MOLSCRIPT and RASTER3D (Kraulis, 1991; Merrit & Murphy, 1994).

A crucial role in the MN12H2−P1.16 peptide complex is played by Asp-182. The loss of approximately 16.6 kJ mol^{-1} in Gibbs free energy of the antibody−peptide 4 complex ($\Delta G° = -25.9$ kJ mol^{-1} at 4 °C) suggests that this residue is involved in the formation of a salt bridge with the antigen binding site of MN12H2. The crystal structure of the MN12H2 Fab−peptide 1 complex shows an interaction of the carboxylate group of Asp-182 and the imidazolium nitrogen Nϵ2 of a histidine residue of the MN12H2 light chain (van den Elsen *et al*., 1997) as is shown in detail in Figure 5. Interestingly, these findings parallel earlier suggestions in the mechanism of the observed increase of endemic meningococcal disease in England and Wales since 1981. This increased incidence of infection by group B meningococci was associated with the occurrence of an *N. meningitidis* escape mutant (strain MC58). A single base change in the *porA* gene of this mutant strain resulted in a D to N amino acid change. Monoclonal antibodies with P1.16 specificity did not react with peptides that correspond to the altered epitope and were not able to promote complement-mediated bactericidal killing of isolates of the mutant (McGuinness *et al*., 1991).

Candidate counterpart residues for salt bridging with Asp-182 in the MN12H2 combining site are histidine, arginine, and lysine. Approximate pK_a values of these residues are 7 (histidine), 10 (lysine), and 11 (arginine). The observed pH profile with an approximate midpoint pH value of 8.5 (Figure 4) most probably reflects the change in the ionization state of a histidine residue from the MN12H2 combining site that is involved in the interaction with the peptide. As stated above this interaction is confirmed by X-ray analysis of the complex (van den Elsen *et al*., 1997). The formation of a salt link is expected to cause an increase of the pK_a value of

all three positively charged candidate residues. pK_a values of 8.0 and higher are not unusual for histidine residues (Bos *et al*., 1989). Therefore, it is most unlikely for Asp-182 to form a salt link with a lysine or an arginine residue.

However, positively charged residues that are not involved in a charge interaction may undergo an acidic shift of their pK_a value when exposed to a hydrophobic environment. For instance, a mutant T4 lysozyme has been described in which a buried lysine residue had a pK_a value of 6.5 (Dao-Pin *et al*., 1991). To exclude an acidic pK_a shift effect between pH 8 and pH 10 of the Lys-181 residue adjacent to Asp-182, the pH dependence of the binding of peptide 2 (Ac-T**X**DTNNNLC-NH_2; X = norleucine) by MN12H2 was determined (Figure 4). Although there is a difference in affinity of MN12H2 for peptides 2 and 1, both reveal an identical pH profile. Similar results were obtained when the Lys-181 residue was exchanged by an arginine residue (pK_a = 11, not shown).

According to the results from a previous study it is unlikely that the observed decrease in affinity between pH 8 and pH 10 can be ascribed to denaturation of MN12H2 (Jiskoot *et al*., 1991c). The antibody molecule shows no significant change in conformation in the pH range between 8 and 10. The collapse in K_a at pH's higher than 10 is presumably caused by protein denaturation. Stability experiments revealed that exposure of MN12H2 to pH >10.5 for 2 h (duration of a binding experiment) caused irreversible loss of affinity of the antibody to peptide 1. The peptide remained unaffected after alkali treatment.

The huge loss of vibrational modes upon formation of the MN12H2−peptide complex, revealed by Sturtevant's analysis, can be ascribed to the loss of degrees of freedom of the side chains, so-called "side chain freezing" of both peptide and the binding pocket. Because the ligand molecule is a peptide with no fixed conformation in solution, there are also backbone contributions involved. Contributions to the loss of vibrational entropy due to conformational changes of the backbone of MN12H2 (induced fit) can only be discriminated when three-dimensional structures of the complex, free antibody, and free ligand are available. Combined loss of conformational entropy resulting from the fixing of peptide 1 and of the side chains in the binding pocket of MN12H2 [ΔS_u(vib) = −326 J K^{-1} mol^{-1}; Table 2] costs 48 kJ mol^{-1} in unitary Gibbs free energy (298 K). This effect is largely offset by the gain in entropy from the release of structured water around hydrophobic groups in the binding pocket [ΔS_u(hydro) = 246 J K^{-1} mol^{-1}), thereby favoring binding by 100 kJ mol^{-1}. We expect the increase of the hydrophobic components partly to be the result of an enhanced interaction of MN12H2 with the fluorescent label in all linear peptide complexes.

Although binding studies with the linear P1.16 epitope mimicking peptide reveal high-affinity binding by MN12H2, the antibodies obtained from linear synthetic peptides showed only low response against PorA in its native conformation (van der Ley *et al*., 1991). Consequently, these antibodies did not have any bactericidal activity. These results are in agreement with studies concerning peptides derived from proteins such as lysozyme, influenza hemagglutinin, and meningococcal PorA, showing improvement of antigenic or immunogenic properties by disulfide cyclization (Arnon *et al*., 1971; Müller *et al*., 1990; Christodoulides *et al*., 1993).

Immunogenicity of these conformationally restricted peptides might be related to the reduced dampening of vibrational contributions to the thermodynamic parameters for cyclic peptides, as revealed from our binding studies with "head-to-tail" cyclized peptides. The vibrational component of ΔG_u is 45−59 kJ mol^{-1} more favorable for the cyclic peptide (C2) compared to the linear peptides (Tables 2 and 3). These reduced unfavorable contributions to the binding can be explained by the decreased intrinsic flexibility of cyclic peptides compared to linear peptides.

Calculation of the nonpolar bsa reveals that there is a significant loss of bsa in the MN12H2−peptide C2 complex (125 $Å^2$) compared to the complexes with linear peptides (Table 1). The increased mobility of the label in the bound state and the small nonpolar bsa value suggest a decrease of the assumed interaction of the label with the antigen binding site as described for the linear peptides. This hypothesis is furthermore supported by Sturtevant's analysis of the binding data with the cyclic peptide (Table 3), which showed that the hydrophobic component of the Gibbs free energy (ΔG_u) of binding is 49−62 kJ mol^{-1} more favorable for the linear peptides compared to C2.

Comparison of our binding data with those obtained in *in vivo* studies (Hoogerhout *et al*., 1995), using a series of 18 different cyclic peptides with ring sizes varying from 7 to 17 amino acid residues, suggests a correlation between binding of MN12H2 to cyclic peptides and the capability of these peptides to elicit bactericidal antibodies. Only the two peptides with a large ring size (15−17 residues) show high-affinity binding by MN12H2 (e.g., peptides C2 and C3) and induction of complement-mediated lysis of meningococci. Apparently, the ring size of the 7−13 residue cyclic peptides is too tight to have enough conformational freedom to mimic the surface loop epitope. The relatively increased conformational freedom, related to the large ring size (peptides C2 and C3), might facilitate the peptide to fold into a few preferable low-energy conformations, succesfully mimicking the native epitope structure.

REFERENCES

Arnon, R., Maron, E., Sela, M., & Anfinsen, C. B. (1971) *Proc. Natl. Acad. Sci. U.S.A. 68*, 1450−1455.

Bentley, K. L., Thompson, L. K., Klebe, R. J., & Horowitz, P. M. (1985) *BioTechniques 3*, 356−366.

Borea, P. A., Varani, K., Guerra, L., Gilli, P., & Gilli, G. (1992) *Mol. Neuropharmacol. 2*, 273−281.

Borea, P. A., Dalpiaz, A., Varani, K., Guerra, L., & Gilli, G. (1995) *Biochem. Pharmacol. 49*, 461−469.

Bos, O. J. M., Labro, J. F. A., Fisher, M. J. E., Wilting, J., & Janssen, L. H. M. (1989) *J. Biol. Chem. 264*, 953−959.

Brugghe, H. F., Timmermans, J. A. M., van Unen, L. M. A., ten Hove, G. J., van de Werken, G., Poolman, J. T., & Hoogerhout, P. (1994) *Int. J. Pept. Protein Res. 43*, 166−172.

Chotia, C. (1974) *Nature 248*, 338−339.

Christodoulides, M., McGuinness, B. T., & Heckels, J. E. (1993) *J. Gen. Microbiol. 139*, 1729−1738.

Dao-Pin, S., Anderson, D. E., Baase, W. A., Dahlquist, F. W., & Matthews, B. W. (1991) *Biochemistry 30*, 11521−11529.

Davies, D. R., Padlan, E. A., & Sherrif, S. (1990) *Annu. Rev. Biochem. 59*, 439−473.

Derderian, E. J., & MacCrury, T. B. (1981) *J. Dispersion Sci. Technol. 2*, 345−358.

de Smidt, J. H., & Crommelin, D. J. A. (1991) *Int. J. Pharmacol. 77*, 261−265.

Eisenberg, D., Schwartz, E., Komaromy, M., & Wall, R. (1984) *J. Mol. Biol. 179*, 125−142.

Gibson, A. L., Herron, J. N., He, X.-M, Patrick, V. A., Mason, M. L., Lin, J.-N., Kranz, D. M., Voss, E. W., Jr., & Edmundson, A. B. (1988) *Proteins 3*, 155−160.
Gilli, P., Ferretti, V., Gilli, G., & Borea, P. A. (1994) *J. Phys. Chem. 98*, 1515−1518.
Gurney, R. W. (1953) *Ionic Processes in Solution*, p 89, McGraw-Hill, New York.
Herron, J. N. (1984) in *Fluorescein Hapten: An Immunological Probe* (Voss, E. W., Ed.) pp 49−76, Boca Raton, FL.
Herron, J. N., & Voss, E. W., Jr. (1981) *J. Biochem. Biophys. Methods 5*, 1−17.
Herron, J. N., Kranz, D. M., Jameson, D. M., & Voss, E. W., Jr. (1986) *Biochemistry 25*, 4602−4609.
Herron, J. N., Terry, A. H., Johnston, S., He, X.-M., Guddat, L. W., Voss, E. W., Jr., & Edmundson, A. B. (1994) *Biophys. J. 67*, 2167−2183.
Hess, W., & Klein, R. (1984) *Prog. Colloid Polym. Sci. 63*, 174−180.
Hoogerhout, P., Donders, E. M. L. M., van Gaans-van den Brink, J. A. M., Kuipers, B., Brugghe, H. F., van Unen, L. M. A., Timmermans, H. A. M., ten Hove, G. J., de Jong, A.P. J. M., Peeters, C. C. A. M., Wiertz, E. J. H. J., & Poolman, J. T. (1995)-*Infect. Immun. 63*, 3473−3478.
Jiskoot, W., Hoogerhout, P., Beuvery, E. C., Herron, J. N., & Crommelin, D. J. A. (1991a) *Anal. Biochem. 196*, 421−426.
Jiskoot, W., Van Hertrooij, J. J. C. C., Hoven, A.-M. V., Klein Gebbinck, J. W. T. M., Van der Velden-de Groot, T., Crommelin, D. J. A., & Beuvery, E. C. (1991b) *J. Immunol. Methods 138*, 273−283.
Jiskoot, W., Bloemendal, M., Van Haeringen, B., Van Gondelle, R., Beuvery, E. C., Herron, J. N., & Crommelin, D. J. A. (1991c) *Eur. J. Biochem. 201*, 223−232.
Kauzman, W. (1959) *Adv. Protein Chem. 14*, 1−63.
Kraulis, P. J. (1991) *J. Appl. Crystallogr. 24*, 946−950.
Makhatadze, G. I., & Privalov, P. L. (1990) *J. Mol. Biol. 213*, 375−384.
McGuinness, B., Barlow, A. K., Clarke, I. N., Farley, J. E., Anilionis, A., Poolman, J. T., & Heckels, J. E. (1990) *J. Exp. Med. 171*, 1871−1882.
McGuinness, B., Clarke, I. N., Lambden, P. R., Barlow, A. K., Poolman, J. T., Jones, D. M., & Heckels, J. E. (1991) *Lancet 337*, 514−517.
Merrit, E. A., & Murphy, M. E. (1994) *Acta Crystallogr. D50*, 869−873.
Mukkur, T. K. S. (1980) *Trends Biochem. Sci.*, 72−75 (March).
Müller, S., Plaué, S., Samama, J. P., Valette, M., Briand, J. P., & Van Regenmortel, M. H. V. (1990) *Vaccine 7*, 325−328.
Murphy, K. P., & Freire, E. (1995) in *Pharmaceutical Biotechnology, Vol. 7: Physical methods to characterize pharmaceutical proteins* (Herron, J. N., Jiskoot, W., & Crommelin, D. J. A., Eds.) pp 219−241, Plenum, New York.
Murphy, K. P., Xie, D., Garcia, K. C., Amzel, L. M., & Freire, E. (1993) *Proteins 15*, 113−120.
Murphy, K. P., Freire, E., & Paterson, Y. (1995) *Proteins 21*, 83−90.
Omelyanenko, V. G., Jiskoot, W., & Herron, J. N. (1993) *Biochemistry 32*, 10423−10429.
Pimentel, G. C., & McClellan, A. L. (1971) *Annu. Rev. Phys. Chem. 22*, 347−385.
Pinckard R. N. (1986) in *Handbook of Experimental Immunology, Vol. 1: Immunochemistry* (Weir, D. M., Ed.) 4th ed., pp 17.1−17.23, Blackwell Scientific Publications, Oxford, U.K.
Privalov, P. L., & Makhatadze, G. I. (1990) *J. Mol. Biol. 213*, 385−391.
Rose, G. D., Geselowitz, A. R., Lesser, G. J., Lee, R. H., & Zehfus, M. H. (1985) *Science 229*, 834−838.
Ross, P. D., & Subramanian S. (1981) *Biochemistry 20*, 3096−3102.
Saukkonen, K., Leinonen, M., Abdillahi, H., & Poolman, J. T. (1989) *Vaccine 7*, 325−328.
Sharp, K. A., Nicholls, A., Fine, R. F., & Honig, B. (1991) *Science 252*, 106−109.
Spolar, R. S., Ha, J.-H., & Record, M. T., Jr. (1989) *Proc. Natl. Acad. Sci. U.S.A. 86*, 8382−8385.
Sturtevant, J. M. (1977) *Proc. Natl. Acad. Sci. U.S.A. 74*, 2236−2240.
Van den Elsen, J. M. H., Herron, J. N., Hoogerhout, P., Poolman, J. T., Boel, E., Logtenberg, T., Wilting, J., Crommelin, D. J. A., Kroon, J., & Gros, P. (1997) *Proteins* (in press).
Van der Ley, P., Heckels, J. E., Virji, J., Hoogerhout P., Poolman J. T. (1991) *Infect. Immun. 59*, 2963−2971.
Wei, A.-P., & Herron, J. N. (1993) *Anal. Chem. 65*, 3372−3377.
Wilson, I. A., & Stanfield, R. L. (1993) *Curr. Opin. Struct. Biol. 3*, 113−118.

BI9700431